First Middle East Conference on Smart Monitoring,
Assessment and Rehabilitation of Civil Structures
8 – 10 February 2011, Dubai, UAE

SMAR 2011

GFRP retrofitted RC frames with columns subjected to high axial stresses

K. D. Dalgic[1], M. Ispir[2], O. Ozel[2], A. Ilki[2]

[1] Istanbul Kultur University, Istanbul, Turkey
[2] Istanbul Technical University, Istanbul, Turkey

ABSTRACT: In developing countries, many existing RC (reinforced concrete) frame buildings are vulnerable against earthquakes due to typical deficiencies such as low strength concrete, insufficient confinement, insufficient joint details and lap splices, and insufficient bond between smooth bars and low strength concrete. Considering the huge stock of this type of deficient existing buildings, research on economical and practical retrofitting methods is urgently needed. In this study, the efficiency of a practical seismic retrofit method in terms of external confinement of columns of typical low quality RC frames is investigated by testing one reference and one retrofitted half-scale flexure-critical RC frames under reversed cyclic lateral loads. Before retrofit design, some material tests were also performed including tensile tests of GFRP (glass fiber reinforced polymer) sheets and compression tests of GFRP confined concrete cylinders. The test frames were constructed with low strength concrete (7-11 MPa) and smooth plain reinforcing bars. The spacing of column stirrups was intentionally designed as 300 mm for reflecting existing frames with insufficient stirrups. The columns of one of the specimens were retrofitted through external confinement. For external confinement of columns, low-density GFRP sheets were used. The frames were tested under simulated seismic loading at the presence of high column axial loads (~60% of axial load carrying capacity). The efficiency of the retrofitting method is evaluated by comparing several quantitative parameters (strength, ductility, energy dissipation, etc.) obtained from tests of reference and retrofitted frames. Furthermore, a simple non-linear seismic performance analysis is carried out for assessing the behavior of GFRP retrofitted frame. At the end of the analysis a satisfactory agreement is found between the predicted and observed behaviors of the retrofitted frame specimen.

1. INTRODUCTION

Although some experimental studies were carried out to investigate the behavior of FRP retrofitted columns under both axial and lateral reversed cyclic loads; Yalcin et al., (2008), Verderame et al., (2008), Realfonzo and Napoli, (2010), there is a lack of experimental data on rectangular columns having some deficiencies such as low strength concrete, insufficient confinement, and plain longitudinal reinforcement bars. These deficiencies can cause significant reductions in strength and ductility. In addition, there are only few experimental studies on FRP retrofitted RC frames; Rocha et al., (2004), Pinto and Taucer, (2006).

In this study, low density biaxial GFRP sheets were used to retrofit the columns of a RC test frame by means of external confinement of columns in transverse direction. The sheets were bonded on columns using anionic high-molecular-weight polyurethane dispersion rather than an epoxy based adhesive. One reference and one retrofitted half scale RC frame were tested under combined action of axial and reversed cyclic lateral loads. Furthermore to assess the confinement efficiency of this low density GFRP sheet, compression tests were carried out on low strength confined concrete cylinders as well. In addition, an analytical study is also carried out to predict the nonlinear behavior of retrofitted RC frame taking into account the confined concrete stress-strain relationships obtained in this study.

2. EXPERIMENTAL WORK

2.1 Compression tests

In order to investigate the efficiency of confinement with low density GFRP sheets, a series of confined concrete cylinder tests were performed. Low strength concrete cylinder specimens externally confined by GFRP sheets were tested under uniaxial compressive stresses. In order to detect the influence of the axial stiffness of the GFRP jacket on the compression behavior, specimens were jacketed externally with 2, 4 and 6 plies of GFRP sheets. Thus, stress-strain relationships of GFRP confined concrete and confining efficiency in terms of strength and deformability were obtained for various levels of strengthening.

2.1.1 Material properties

For external confinement of cylinders, bidirectional low density (250 g/m^2 in one direction) GFRP sheets were used. The warps were in horizontal direction during jacketing application. Elasticity modulus, tensile strength and ultimate tensile strain of the glue coated GFRP sheets are; 38.1 (35.2) GPa, 1000 (844) MPa and 0.026 (0.024) mm/mm in warp direction. While the values given in brackets are the experimental tensile test results obtained by the authors, the ones out of the brackets are reported by the manufacturer. It should be noted that the mechanical properties may differ in weft direction. The glue has the content of anionic high-molecular-weight polyurethane dispersion and it is used by mixing with a thickener. The glue used in the study is cheaper than the epoxy based adhesives and it does not have any harmful effect for human health. For representing the concrete quality of the RC frames to be tested in the second part of this study, the standard cylinders to be tested under compression were cast intentionally using low strength concrete in three batches. Compressive strengths and elasticity moduli of each concrete batch are given in Table 1.

Table 1. Compressive characteristics of concrete cylinders.

Batch	Uniaxial compressive strength (MPa)	Elasticity modulus experimental (MPa)	Elasticity modulus* (MPa) (Ispir et al. 2010)
n1	10.6	19560	17500
n2	8.8	18675	16200
n3	7.8	16055	15500

*calculated using equation proposed by Ispir et al. (2010).

$$E_c = 4630\sqrt{f'_c} + 2370(MPa)$$

2.1.2 Test setup

A total of six confined cylinder specimens were tested by using an Amsler testing machine of 5000 kN load capacity. While load was measured by a load cell of 1000 kN capacity, axial shortening was measured by two strain gages and two LVDTs (linear variable differential transducers) aligned vertically. In addition, transverse strains were measured by two strain gages bonded horizontally on the mid-height of the specimen with 180 degree intervals around perimeter. Load and deformation datum were transferred to a data logger and saved by a computer. The test setup with measurement system and a deformed specimen is presented in Figure 1.

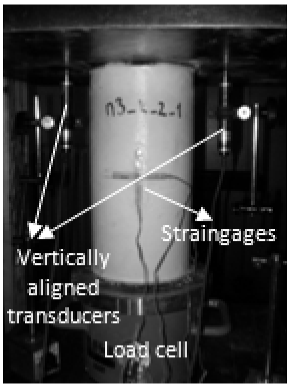

Figure 1. Compression test setup for confined cylinder specimens and a deformed specimen after test.

2.1.3 Test results

The test results are given in Table 2. In Table 2, ε_{co} is the unconfined axial strain at unconfined strength level f_{co}, ε_{cc} is the ultimate axial strain of confined concrete at confined strength level f_{cc} and ε_{ch} is the maximum transverse strain that could be measured. Consequently, ε_{ch} does not always correspond to ultimate state. During compression tests, it was observed that ε_{ch} reached approximately 70% of the ultimate uniaxial tensile strain capacity of GFRP sheets.

As seen in this table, a slight strength increase (~10%) was obtained for the specimens jacketed with 2 plies of GFRP sheets. The compressive strength increased 60 and 90% for the specimens jacketed with 4 and 6 plies of GFRP sheets, respectively. On the other hand, deformability capacity increased 5.5 times for specimens jacketed with 2 plies of GFRP sheets, 7.8 times for 4 plies cases, and 8.5 times for 6 plies cases on average. Deformability was determined as the ratio of ultimate confined concrete compressive strain to the 0.002 strain, which is assumed as the unconfined concrete compressive strain corresponding to the unconfined strength.

In addition, strength and deformability capacities were also predicted by the model proposed by Ilki et al. (2004) given in Equation 1. In Equation 1; f_{cc}, f_{co}, f_{lmax} shows GFRP confined concrete compressive strength, unconfined concrete compressive strength and maximum lateral pressure GFRP jacket can apply to the concrete core, respectively. As seen in Table 2, there is a satisfactory agreement between experimental data and analytical predictions. Normalized axial stress-axial strain and normalized axial stress-transverse strain relationships are given in Figure 2. In this figure, it is clear that at large compressive strains, strain gages bonded on the GFRP jacket did not perform accurately due to relative displacement of inner concrete core with respect to GFRP jacket.

Table 2. Summarized confined concrete test results.

Specimen	Batch of strength	Number of plies	f_{co} (MPa)	f_{cc} (MPa) *Experiment*	f_{cc} (MPa) *Ilki et.al*	ε_{co}	ε_{cc} *Experiment**	ε_{cc} *Ilki et.al*	ε_{ch}	f_{cc}/f_{co}	$\varepsilon_{cc}/\varepsilon_{co}$
n3_k_2_1	n3	2	7.8	8.7	10.8	0.002	0.0172	0.020	0.0190	1.1	6.5
n3_k_2_2	n3	2	7.8	8.7	10.8	0.002	0.0170	0.020	0.0220	1.1	4.5
n2_k_4_1	n2	4	8.8	14.5	15.5	0.002	0.0250	0.026	0.0177	1.6	8.0
n2_k_4_2	n2	4	8.8	14.1	15.5	0.002	0.0240	0.026	0.0180	1.6	7.5
n1_k_6_1	n1	6	10.6	19.7	21.1	0.002	0.0299	0.029	0.0177	1.9	9.0
n1_k_6_2	n1	6	10.6	20.1	21.1	0.002	0.0320	0.029	0.0178	1.9	8.0

*Experimental strain values in this table were obtained by LVDTs in 300 mm gage length.

$$f_{cc} = f_{co}\left[1 + 2.4\left(\frac{f_{l\max}}{f_{co}}\right)^{1.2}\right] \tag{1a}$$

$$\varepsilon_{cc} = \varepsilon_{co}\left[1 + 20\left(\frac{f_{l\max}}{f_{co}}\right)^{0.5}\right] \tag{1b}$$

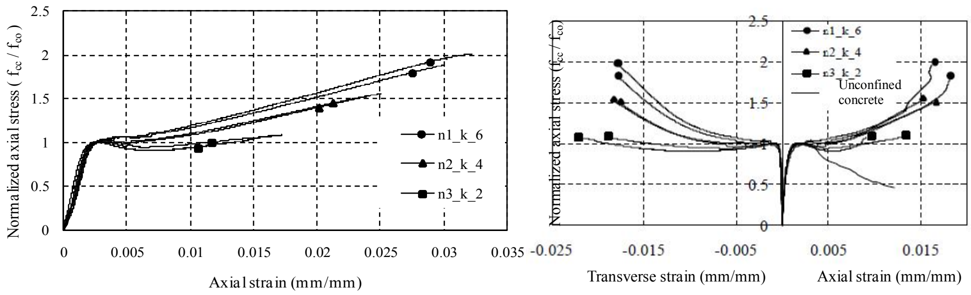

(a) *(b)*

Figure 2. Normalized stress - strain relationships obtained by *(a)* LVDTs and *(b)* strain gages.

2.2 *RC frame tests under combined action of column axial compression and reversed cyclic lateral loads*

To investigate the effect of the retrofitting on the behavior of RC frames with rectangular columns, two half scale RC frames were tested under axial compressive load and reversed cyclic flexure. The RC frames were constructed with the low strength concrete and plain bars. The columns of one of the RC frames were retrofitted by external confinement of columns in transverse direction using the GFRP sheets aforementioned.

2.2.1 Materials

In this study, plain reinforcing bars were used to represent relatively old existing RC frames. The longitudinal and transverse bar diameters were 16 and 10 mm, respectively. For longitudinal bars, mean yield strength, mean maximum strength and mean fracture strength were 347, 501 and 350 MPa. These values were 357, 455 and 294 MPa for transverse bars, respectively. Concrete used for construction of the frames was similar to that used in compression tests. The compressive strength at around the day of frame tests was determined as 6.75 MPa through standard concrete cylinder (150 x300 mm) tests. The mechanical properties of GFRP sheets are the same as in the case of confined cylinder compression tests.

2.2.2 Specimen characteristics

Frames were designed to be representative of frames of the existing structures. Figure 3 illustrates the cross sections and reinforcement detailing of specimens. To reflect the axial stress states of actual columns in existing old type RC frame structures, high level of axial stress (60% of axial load capacity) was applied on columns intentionally. This situation may be described with a loading state, which is located on the upper side of balanced state on P-M interaction curve. In this state, it is expected that concrete crushes before the reinforcing bars on the tensile side of the section yield. Eventually, column sections were designed as 200x250 mm and axial load was 200 kN per column. Beam sections were dimensioned as 200x325 mm and designed to be stronger than columns for reflecting actual cases and preventing excessive damage on regions other than bottom regions of columns. In other words, bottom region of columns were selected as observation regions during the tests, where damage is expected. In this region, stirrup spacing was selected as 300 mm from the top level of the foundation to 600 mm height along the column. Other parts of the columns and whole length of the beam were over-designed to enforce the damage occur in the damage observation regions.

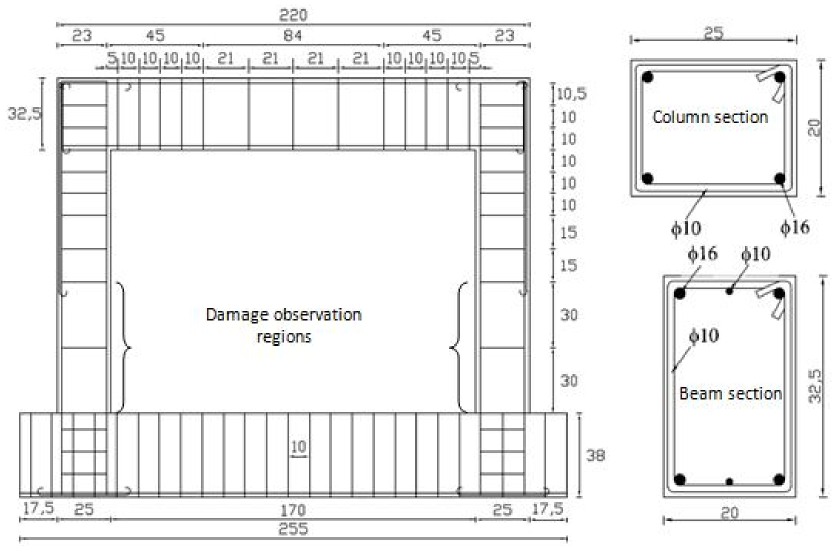

Figure 3. Reinforcement detailing and cross sections of RC frame specimens (dimensions are in cm).

2.2.3 Test setup

In order to assess the behavior of RC frames under seismic loads, frames were tested under reversed cyclic lateral loads at the presence of constant and high column axial stresses. Column axial loads were increased gradually up to 200 kN for each column by means of a tension rope mechanism and from then onwards reversed cyclic lateral load was applied. The same loading pattern was used for both reference and retrofitted frame specimens. Test setup and the lateral load pattern are presented in Figure 4. Frame tests were performed in a displacement controlled manner. Measurement system included LVDTs, post yield type strain gages on reinforcing bars, two load cells with 1000 kN load capacity and the internal load cell and displacement transducer of the hydraulic actuator. The data picked up through this measurement system was transferred to the switch box at first and later to the data logger. To determine the average section curvatures on columns, LVDTs with 25 mm gage length were installed on each side of the columns in loading plane. In addition, a LVDT with 200 mm gage length was installed to measure the top displacement of the frame. For checking the foundation rotation and translation, LVDTs with 25 mm gage length were used. On the other hand, out of plane behavior of frame specimen was checked by two LVDTs with 50 mm gage length. The LVDTs showed that these displacements did not have a remarkable effect on the behavior until very large drift ratios reached during the tests.

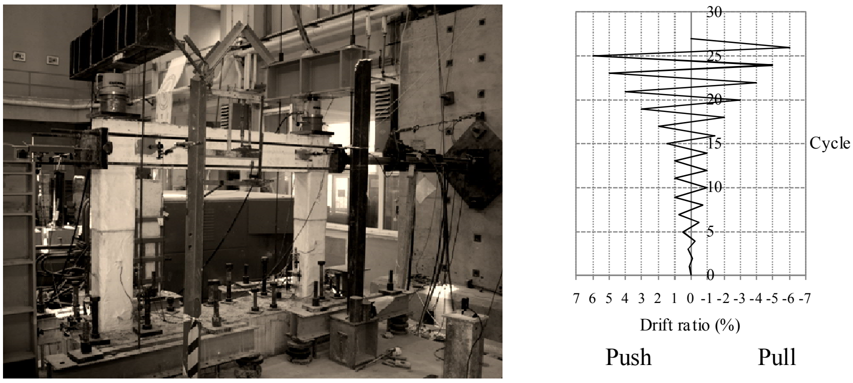

Figure 4. Test setup and displacement history.

2.2.4 Retrofit design

Retrofit design was made through a nonlinear section analysis. For obtaining moment-curvature relationships of GFRP confined concrete, XTRACT (v.3.0.3) section analysis program was utilized. For the stress-strain relationships of concrete columns confined by GFRP, Ilki et al. (2004) stress-strain model, which was shown to be capable of making successful predictions for many experimental results for cylinder or rectangular columns, was used. The moment-curvature relationships obtained from the section analyses exhibited that the number of GFRP plies should be at least eight for a ductile failure mechanism. For the ductile failure mechanism, while an enhancement of axial deformability for concrete is expected due to external confinement of the columns, the reinforcing bars are expected to reach yield strength before crushing of concrete on the compression side of section.

2.2.5 Test results

The frame test results are presented in terms of normalized lateral load (P/P_{max}) and drift ratio in Figure 5. P is the lateral load acting on the specimens at each step of loading, while P_{max} is the maximum load resisted by the reference specimen. As seen in Figure 5, while the lateral load capacity of the retrofitted specimen is enhanced slightly, there is a very remarkable enhancement in ductility. Cumulative energy dissipation was calculated as summation of the areas under the load-displacement cycles. On the other hand, the normalized stiffness was calculated for each cycle as the ratio of stiffness obtained in that cycle to the maximum stiffness obtained from the first cycle. The change in cumulative energy dissipation and normalized lateral stiffness by the drift ratio are given in Figure 6. The ductility ratios of the specimens were calculated as the ratio of the displacement at 85% of the peak lateral load on the descending branch of the load-displacement relationship to the displacement at the peak lateral load (Table 3). It was assumed that 15% strength loss in lateral direction is the limit for load carrying capacity representing the ultimate state.

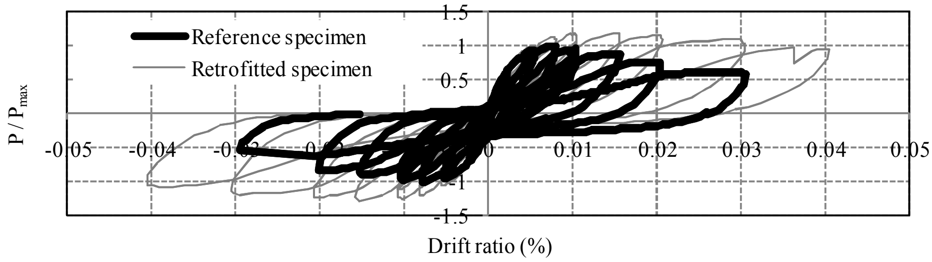

Figure 5. Normalized lateral load versus drift ratio diagram.

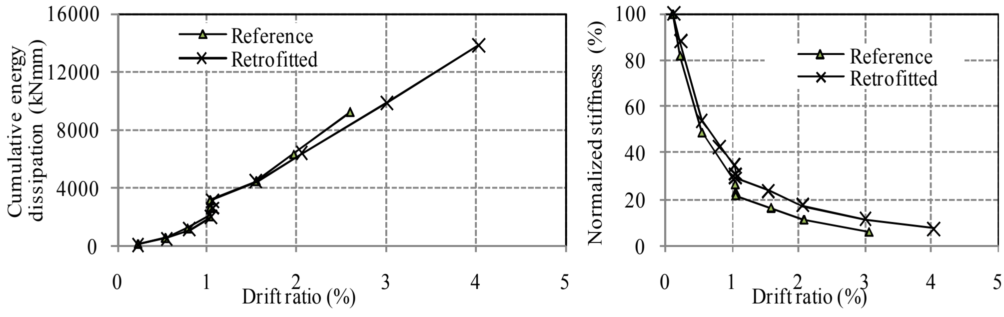

(a) *(b)*

Figure 6. Variation of *(a)* cumulative energy dissipation, (*b)* normalized stiffness degradation.

A more justified comparison in terms of energy dissipation can be made at same levels of strength loss for each specimen. The reference specimen and the retrofitted specimen suffered 40 and 20% strength loss, respectively at the end of the tests. The reference and retrofitted specimens lost identical portions of their lateral strengths as 1 and 4% drift ratios, respectively. Thus, it can be clearly seen that the energy dissipation of the retrofitted specimen at 4% drift ratio is significantly higher than that of reference specimen at 1% drift ratio.

Table 3. Displacement ductility.

Frame	Top displacement at applied max. lateral load (mm) (δ_{max})	Top displacement at 85% of the applied max. lateral load (mm) ($\delta_{0.85}$)	Displacement ductility $\delta_{0.85}$/ δ_{max}
Reference	10.44	13.90	1.33
Retrofitted	20.18	40.35	1.99

3. ANALYTICAL CONSIDERATION

Using Ilki et al. (2004) stress-strain model for GFRP confined concrete; a section analysis was performed to obtain a theoretical moment-curvature relationship for the retrofitted frame. Section analysis was carried out by XTRACT (v.3.0.3) section analysis program and then load-top displacement curve of the retrofitted frame was obtained through a nonlinear pushover analysis. Plastic hinge length was assumed as the half of the effective depth of the column section. Furthermore, the elastic deformations outside the plastic hinge zones were also taken into account during calculation of theoretical displacements. Experimental and theoretical load-top displacement envelope curves are given in Figure 7. As seen, both lateral strength and displacement characteristics are predicted quite accurately. It should be noted that the last point of the theoretical curve corresponds to the ultimate compressive strain of confined concrete at compression side of section.

4. CONCLUSIONS

A practical frame seismic retrofitting method was investigated during this study. The columns of one of the frames, which represented the columns of relatively old type existing RC buildings, were externally confined with low density GFRP sheets. The sheets were bonded on the columns using anionic high-molecular-weight polyurethane dispersion, which is a relatively cheap type adhesive. The retrofitting significantly improved the behavior, particularly in terms of ductility. The nonlinear behavior of the retrofitted frame could be predicted successfully by pushover analysis.

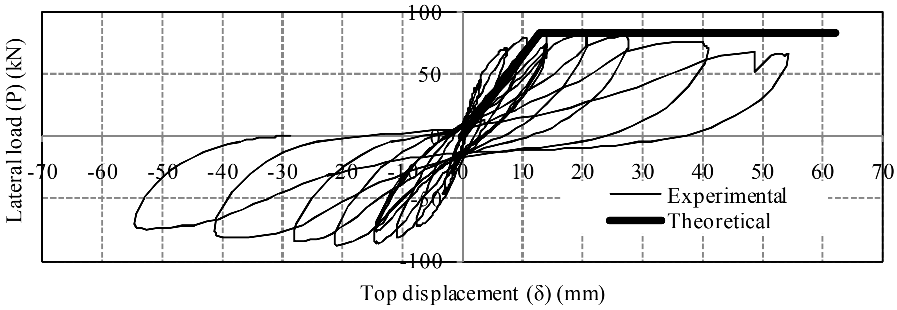

Figure 7. Experimental and theoretical P-δ curves.

ACKNOWLEDGEMENT

The authors would like to acknowledge Msc. Engineer Mr. Orkun Incecik for his invaluable support and effort during experiments and Mr. Gökhan Terlemez for providing most of the materials used in this study. The authors also gratefully acknowledge Mr. Ogün Fırat and Mr. Peter Kühn for their suggestions.

REFERENCES

Ilki, A., Kumbasar, N., and Koc, V., 2004. Low strength concrete members externally confined with FRP sheets, *Structural Engineering and Mechanics*, 18: 167-194.

Ispir, M., Dalgic, K. D., Sengul, C., Kuran, F., Tasdemir, M. A., Ilki, A. 2010. Elasticity modulus of low strength concrete. *International Congress on Advances in Civil Engineering,* Trabzon, Turkey.

Pinto, A. V., Taucer, F., 2006. Assessment and Retrofit of Full-Scale Models of Existing RC Frames. *S.T. Wasti and G. Ozcebe (eds.), Advances in Earthquake Engineering for Urban Risk Reduction,* 353- 367.

Realfonzo, R. and Napoli, A., 2010. Cyclic Behavior of RC Columns Strengthened by FRP and Steel Devices. *Journal of Structural Engineering*, ASCE, 14: 62-71.

Rocha, P., Delgado, P., Costa, A., Delgado, R., 2004. Seismic retrofit of RC frames. *Computers and Structures*, 82:1523-1534.

Verderame, G. M., Fabbrocino, G., Manfredi, G., 2008. Seismic response of r.c. columns with smooth reinforcement. Part II: Cyclic tests. *Engineering Structures*, 30: 2289-2300.

Yalcin, C., Kaya O., Sinangil M., 2008. Seismic retrofitting of R/C columns having plain rebars using CFRP sheets for improved strength and ductility. *Construction and Building Materials*, 22: 295-307.

XTRACT (v.3.0.3) Section Analysis Program, Imbsen Software Systems.